CHANGES IN FLOW DIRECTION AT A POINT CAUSED BY OBSTACLES DURING PASSAGE OF A DENSITY CURRENT

STEPHEN A. MORRIS[1]* AND JAN ALEXANDER[2]
[1] *Department of Earth Sciences, Cardiff University, P.O. Box 914, Cardiff, CF1 3YE, U.K.*
e-mail: stephen.morris@bakeratlas.com
[2] *School of Environmental Sciences, University of East Anglia, Norwich, NR4 7TJ, U.K.*

ABSTRACT: **The flow pattern and sediment character of laboratory density currents partly blocked by bed topography is used to demonstrate how changes in paleocurrent direction through a turbidite at a single site can be explained. These experiments confirm that a relatively small obstacle may affect bed thickness and paleocurrent patterns at considerable distances away from obstacles. Density currents generated by a lock-exchange mechanism spread radially across the tank floor and were partially blocked by a wedge-shaped obstacle with steep face (scarp) facing upstream. When the body of the current impinged on the obstacle, a thickened region of the flow developed upstream of the scarp, with increased entrainment of ambient fluid above it. The upflow edge of the thickened region was at a small angle to the obstacle front and propagated rapidly upflow and to the sides of the obstacle. Internal flow vectors observed with thread flags were radial from the lock before the head reached the obstacle. After the head passed the obstacle, flow vectors in the region of thickened flow upstream and to the sides of the obstacle were reoriented nearly parallel to the obstacle scarp. Thus flow vector at a point rotated by as much as 45° during passage of the current. The deposits of sediment-laden density currents thickened in the region of observed flow thickening because of an increased particle flux to the bed caused by velocity reduction. The upflow limit of the influence of the obstacle on deposition is marked by an abrupt increase in the thickness of the deposits. This area of thickening occurs in an area where the flow is accumulative.**

INTRODUCTION

There is considerable evidence that basin topography controls turbidite distribution, character, and paleocurrent patterns (e.g., van Andel and Komar 1969; Hiscott and Pickering 1984; Pickering and Hiscott 1985; Marjanac 1990; Kneller et al. 1991; Pickering et al. 1992; Clayton 1993; Agirrezabala and García-Mondéjar 1994; Haughton 1994, 2000; Sinclair 1994, 2000; Chikita et al. 1996; Lebreiro et al. 1997; Morris et al. 1998; Kneller and McCaffrey 1999; Bursik and Woods 2000). Many of these case studies document divergence between paleocurrent directions interpreted from erosional sole structures and from ripple cross lamination or grain fabrics within single beds at one site (e.g., Marjanac 1990; Haughton 1994; Kneller et al. 1991; Kneller et al. 1995). Variations in flow direction at a point through the duration of a density-current event have been explained by flow stripping (Piper and Normark 1983), turbulence (Allen 1982), lobe and cleft development (Morris 1998; Kneller and Buckee 2000), flows from different sources passing over same point in quick succession (Anderson 1965), flow reflection (e.g., Pantin and Leeder 1987; Edwards et al. 1994; Kneller et al. 1995), and deflection (e.g., Clayton 1993; Haughton 1994). This paper aims to demonstrate an additional explanation (partial deflection) for variation in flow direction at a point by presenting observations of four experimental density currents.

Kneller and McCaffrey (1999) discussed the effects of flow non-uniformity on depositing turbidity currents approaching a basin-bounding slope. They suggested that in a quasi-steady current the magnitude of non-uniformity dictates suspended-load fallout rate and therefore bed thickness and facies variations. Many natural density currents and the laboratory currents described here are strongly non-uniform. Kneller and McCaffrey (1999) also showed that the response of stratified flows to topography is more complicated than that of well-mixed flows.

Pickering and Hiscott (1985) described turbidites in the Cloridorme Formation (Quebec) where paleocurrent direction reversed within single beds and explained this by individual currents undergoing one or more reflections of 180°. Pantin and Leeder (1987) proposed a model for reverse flow in a turbidity current following its interaction with an adverse slope and confirmed the findings with a series of experiments. They showed that the nose of a current impinging on an adverse ramp forms a ''hump,'' which then moves in the reverse direction to the flow. The hump breaks down into a series of internal solitons that propagate along the top of the residual flow. They concluded that the reduced forward velocity associated with the passage of the solitons would lead to the deposition of mud drapes. Edwards et al. (1994) designed a series of experiments to investigate the effects of an adverse ramp-type obstruction on the motion of density currents. They showed that the reflected bores are stronger when there is a large ratio between the depth of the reverse flow and the residual forward flow. This ratio is largest when more proximal parts of the flow impinge upon steeper ramps. Kneller et al. (1995) suggest that the primary flow in a laterally restricted basin cuts sole structures and may fill them with sand. Later when the primary spreading current interacts with the restricting basin slope, solitary waves that propagate through the body of current can lead to reworking of earlier deposits and can form ripples in upper parts of beds, indicating flow perpendicular to the restricting slope.

In the Rhuddnant Grits Formation (Wales), paleocurrents measured from sole structures and ripple cross-lamination in the same bed diverge less than 30° in a basin where reflection and soliton production was likely. Clayton (1993) attributed the small divergence angle and progressive anticlockwise rotation to deflection caused by currents banking against the basin-bounding slope or the Coriolis effect, or a combination of the two (cf. Woodcock 1990).

Variations in sediment character are recorded in the Tabernas–Sorbas Basin in southeastern Spain (Haughton 2000), where thin-bedded turbidites deposited from flows that interacted with basin topography are distinctly different from those that were deposited from unobstructed turbidity currents. This is shown by reversed current-ripple directions from flows that ''sloshed'' back and forth across the basin floor.

This study arose following experiments (Alexander and Morris 1994; Morris 1998) in which a thickened sediment deposit was observed in the area immediately upflow of an oblique obstacle scarp. The thickened deposit had an orientation that was not parallel to the obstacle scarp, and the experiments reported here investigate the processes of flow interaction immediately upflow of the obstacle that caused this thickening pattern and whether accumulative flow is always the overriding factor controlling deposition or nondeposition when flows interact with obstacles (cf. Kneller and McCaffrey 1999). These experiments demonstrate that partial blocking and deflection of a flow can explain the progressive rotation of current indicators during flow around an obstacle and that sediment character can be affected at a considerable distance away from the obstacle. The density currents flowed over obstacles narrower than the flow width and oriented

* Present address: Baker Atlas GEOScience, Baker Hughes Building, Stoneywood Park North, Dyce, Aberdeen, AB21 7EA, U.K.

JOURNAL OF SEDIMENTARY RESEARCH, VOL. 73, NO. 4, JULY, 2003, P. 621–629
 1527-1404/03/073-621/$03.00

TABLE 1.—*Initial conditions for experimental runs.*

Run number	Tank used in experiment	Initial density of suspension/ brine (kg m^{-3})	Initial sediment concentration (%)	Measured mean grain size (μm)	Initial volume of suspension/ brine in lock (m^3)	Maximum head velocity (ms^{-1})	Shown in Figures
1	Small tank (Fig. 1A)	1222	10	80 S.D. 24.03	1.03×10^{-2}	0.35	2, 3
2	Small tank (Fig. 1A)	1222	10	57 S.D. 17.90	1.03×10^{-2}	0.30	—
3	Large tank (Fig. 1B)	1222	10	80 S.D. 24.03	3.814×10^{-3}	0.24	5
4	Large tank (Fig. 1B)	1074	0	Brine	3.814×10^{-3}	0.20	3, 4

Note: S.D. = standard deviation. Maximum head velocity measured upflow and before current interaction with obstacle scarp. Ambient fluid density = 1000 kg m^{-3}.

at 45° to the mean flow direction. The flows were accumulative in the area immediately upflow of the obstacle but increased deposition may have been due to strongly waning flow (cf. Kneller 1995; Kneller and Branney 1995). The experiments also give some indication of the likely distance over which an obstacle could disrupt the flow and cause deposit variations away from any localized topography.

THE EXPERIMENTS

The experimental runs (Table 1) comprised density currents of sediment suspensions or brine intruding into fresh water and are similar to the experiments described by Alexander and Morris (1994). Two tanks were used, one made of Perspex with a glass floor (1 m × 1 m × 0.17 m, filled to 0.13 m above the sampling platform; Fig. 1A), the other made completely of clear Perspex (1.5 m × 1.5 m × 0.25 m, filled to 0.16 m; Fig. 1B). Different tanks were used because of the availability of measuring apparatus in different locations, but this also allowed the measurement of different aspects of both flow behavior and deposit variations. In both tanks the floor of the lock is a continuation of the tank floor, and the floors were marked with sampling grids with 0.04 m (small tank) and 0.05 m (large tank) spacing. The small tank had a gutter 0.06 m deep near the walls to reduce the influence of currents reflecting from the tank sides.

The currents interacted with topographic features with a height, *h*, approximately 1.5 times flow body thickness, *Z*. Wedge-shape obstacles (Fig. 1C and D, in tanks represented by Fig. 1A and B, respectively) were positioned with the vertical side (scarp) obliquely facing the lock gate at an angle of 45°. The leading corners of the obstacles were 0.28 m (small tank) and 0.35 m (large tank) from the tank wall with lock gate (Fig. 1A and B), and this distance was chosen in order that they interacted with the fully developed current, in an area of relatively steady or slowly declining head velocity: cf. Alexander and Morris (1994) for comparison with similar currents unaffected by obstacles.

In Runs 1, 2, and 3, suspensions of very angular, low-sphericity, silicon carbide grains (density 3220 kg m^{-3}) of two different mean grain sizes formed the density currents (Table 1). The initial density of the suspensions

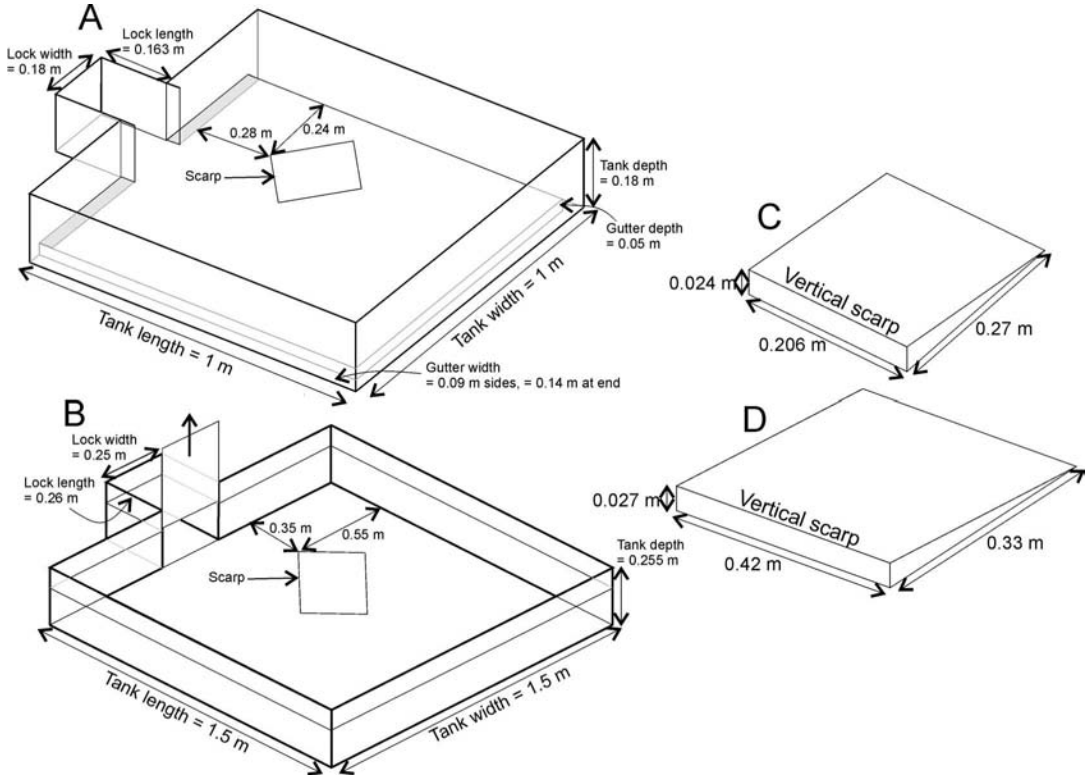

FIG. 1.—Tanks and obstacles used in the experiments. **A)** The small tank is made of Perspex, with a floor built up from sheets of glass to produce a gutter around the corner of the sampling area. The gutter captures the distal, dilute part of the flow and prevents it from reflecting over the deposit of the primary flow. **B)** The large tank is made of Perspex, with a Perspex floor at the same height as the lock floor. The obstacles used in the small (**C**) and large (**D**) tanks are made from Perspex and are scaled to be similar in height to that of the body of flows, thereby causing full or partial blocking.

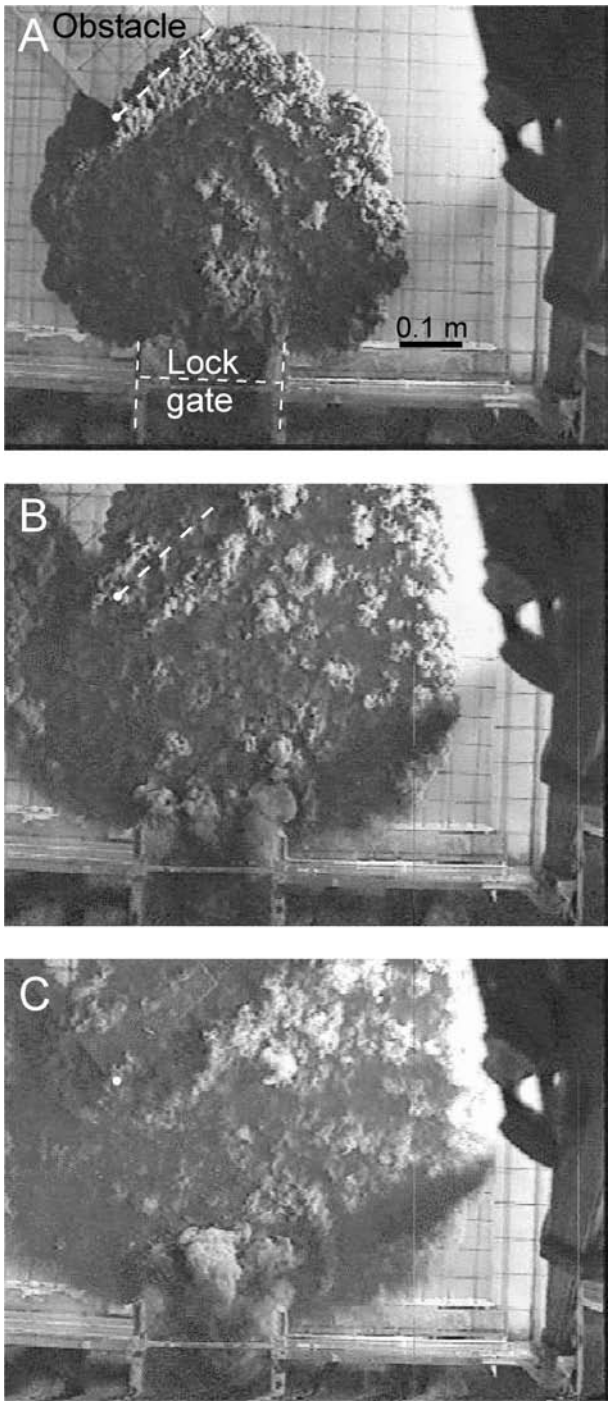

FIG. 2.—Video stills from Run 3 (Table 1) over oblique obstacle C (Fig. 1) at various stages of flow propagation in the small tank. **A)** At $T = 2$ s the head of the flow had just passed the leading corner of the obstacle (denoted by the white dot). The head had reached the downstream corner of the obstacle scarp (denoted by the dotted white line) and was being retarded over the scarp of the obstacle. **B)** By $T = 3$ s, the head on the tank floor had passed the downstream corner of the scarp and had moved down the lee slope of the obstacle. A deep gulf had developed in the head behind the leading corner of the obstacle, and the flow was being retarded over the obstacle. An intense mixing cloud had developed over the body of the flow, at a mean distance of 0.15 m upflow of the obstacle scarp. This cloud had detached from the head of the current and was migrating away from the obstacle scarp in the opposite direction to mean flow, across the still advancing body of the current. **C)** At $T = 4$ s, the flow head, moving to the sides of the lock gate and on top of the obstacle, had almost completely stopped advancing, but the head continued to propagate past the right-hand side of the obstacle. The scarp of the obstacle was now

was the same. The use of such coarse-grained sediment was necessary to ensure that the flow underwent full evolution and deposited most of its sediment within the tank confines and from the primary flow, before interaction with the tank walls. The homogeneous suspension was generated by mixing in the lock with a gridded paddle and released into the tank by removing the lock gate. The suspensions collapsed onto the tank floor and formed dense, opaque undercurrents that were recorded on video, viewing directly down on the tank, to allow accurate measurement of head positions and for calculations of velocity. In experiment Run 3, immediately after all the sediment had settled, the thickness of the unconsolidated deposit was measured on a centimeter-spaced grid with a wire probe coated with petroleum jelly. Sediment adhered to the wire probe and was measured using Vernier calipers (cf. Morris 1998). Sediment mass distribution was obtained by siphoning from tank floor grids and capturing the sediment in preweighed filter papers, which were dried and reweighed.

The brine current (Run 4) allowed observation of the internal behavior of a current as it impinged upon the obstacle. The initial density of the brine was less than that of the particulate suspensions, because this was approaching the limit of salt that could be dissolved effectively in the lock water. Food coloring was added to show the changes in flow thickness as it interacted with the obstacle. Lengths of black cotton thread (0.03 m) were attached to the tank floor in the center of grid squares in the area between the lock and the obstacle and acted as flags that indicated the flow direction. Head positions, changes in body thickness, and changes in localized flow vectors were measured from video recordings. Flow thickness at various positions was measured from video recordings of identical repeat runs with a vertical ruler oriented so as not to disturb the flow (flow parallel).

FLOW BEHAVIOR

Behavior of the Head

On release from the lock (at $T = 0$ s) the dense fluid rapidly decreased in thickness (collapsed) and spread out over the tank floor. In all runs, a distinct flow head developed at $T \approx 1.0$ s (~ 0.08 m thick; e.g., Fig. 2). When the flow head reached the leading corner of the obstacle (at $T = 1.6$ s in Run 3; cf. Fig. 3A) it ''splashed up'' the scarp, causing a localized flow thickening (up to ~ 0.11 m in Run 3; Figs. 2A, 3A). Stationary, rotating mixing billows developed above the thickened area of the flow. These persisted for several seconds after the head passed the obstacle. The height of the thickened area varied little for several seconds (until $T > 4$ s in Run 3). The localized flow thickening started to subside as the tail of the flow approached the area. When the flow advanced around the downstream corner of the obstacle (Figs. 2B, 3A), it was thinner than upstream of the obstacle (at ~ 0.06 m) and lacked a distinct head.

Behavior of the Body

On approaching the obstacle the body of the current was mostly diverted and became thicker in an area upstream of the obstacle. The area of thickened flow spread rapidly sideways across the flow at an angle to both the flow direction and the obstacle scarp (Figs. 2, 3). The head positions show nearly radial propagation from the lock (Fig. 3A, C), followed by retardation over the leading corner of the obstacle. In all runs, the upflow limit

←

visible through the waning billows that had been cast into the ambient fluid during the passage of the head over the obstacle scarp. The mixing cloud over the body had migrated a short distance farther away from the scarp, but its velocity had slowed. After $T = 4$ s, the mixing cloud over the body stopped propagating any farther away from the scarp and on final waning of the flow was swept downstream by the movement of entrained ambient fluid.

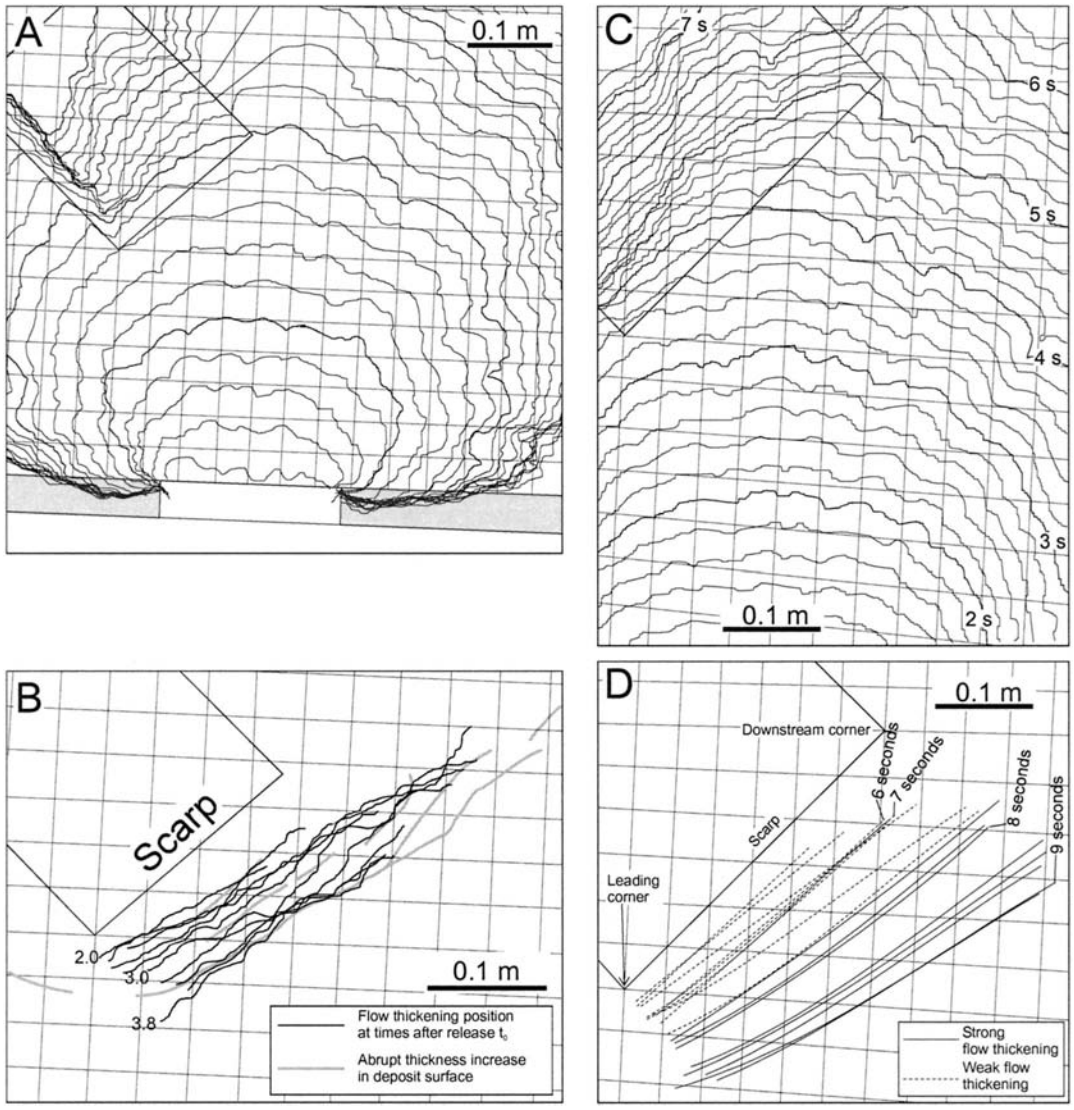

FIG. 3.—Head propagation and deposit variations in Run 1 (A and B), compared with brine current head propagation and body thickening in Run 4 (C and D). Mean flow direction is bottom to top. **A)** Head position at 1 s (bold lines) and 0.2 s intervals (thin lines) traced from the video stills. **B)** The upstream propagation of the thickened body is shown by thin lines. The abrupt thickness increase observed in the corresponding deposits is shown by thicker gray lines. **C)** Head positions of the brine current Run 4, with bold lines at 1 s intervals and thin lines at 0.2 s intervals. **D)** Propagation of the flow thickening in front of the obstacle scarp in Run 4.

of the thickened flow body propagated into the trailing body of the flow and to the side of the obstacle with variable propagation rates (as seen in the irregular spacing of lines in Fig. 3B and D). Deep gulfs developed in the heads of flows as they passed over the leading corner of the obstacles, contributing to acute retardation of the flow behind the obstacle, and short run-out over the obstacle (Fig. 3A). An intense mixing cloud developed over the body of the currents (in Runs 1, 2, and 3) at a mean distance of 0.15 m upflow of the scarp (Fig. 2C). This cloud detached from the head of the current and migrated away from the obstacle upstream, apparently across the body of the current that was continuing to advance towards the obstacle. The cloud front was uneven but assumed an overall linear trend at about 10–15° to the scarp. In Run 1, the mixing cloud front initially (from $T = 2.0$ to 3.2 s) propagated at a steady rate (~ 0.03 ms^{-1}) and then slowed a little to its last recorded stable position at $T = 3.8$ s ($\sim$ 0.11 m from the scarp). On final waning of the current, the mixing cloud was swept downstream. In Run 2, the mixing cloud and flow-thickening front propagated to a greater distance from the scarp than in the coarser-grained equivalent experiment.

Behavior of the Brine Flow

The slightly lower initial density of the brine flow in Run 4 caused the initial head velocity to be less than the particulate flows. When the head reached the leading corner of the obstacle (at $T = 3.3$ s; Fig. 3C) it was about the same thickness as those of the particulate flows. The brine current did not mix so vigorously with the overlying ambient fluid, the head was not disturbed greatly, and a deep gulf did not develop behind the leading corner of the obstacle. The absence of mixing billows over the head may have been a result of a higher Richardson number than in the particulate currents caused by the lower forward velocity, which may have also resulted in a slower rate of ingestion of ambient fluid at the nose. The head was slowed slightly over the scarp of the obstacle but continued to flow at a nearly constant velocity down the slope. The thickened flow upstream of the obstacle was visible as a darker red area in comparison to the normal body thickness. The thickened flow front (recorded at 0.2 s intervals in Fig. 3D) was initially weakly developed (dotted lines in Fig. 3D) and propagated away from the scarp in a nearly parallel orientation. By $T = 7.4$ s,

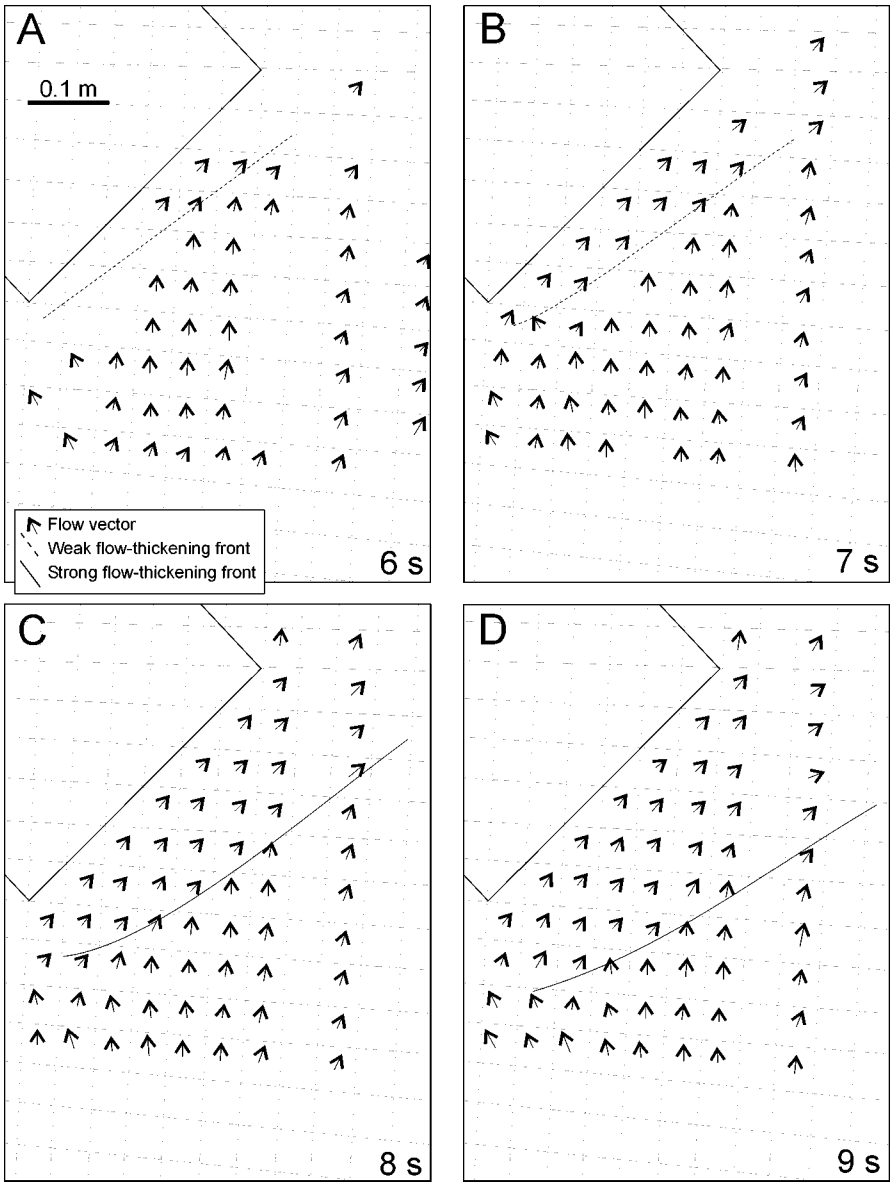

FIG. 4.—Sequence of near-bed flow vectors derived from flags and flow-thickening propagation in the brine flow of Run 4. Some arrows are absent because the flags could not been seen through the turbulent current at certain times. **A)** At $T = 6$ s after release, most flags point away from the lock gate with a slight radial spread. The flow thickening is weakly developed and is marked by a dotted line. Downflow of the flow thickening, the flags are oriented parallel to the obstacle scarp. **B)** At $T = 7$ s, the weakly developed hydraulic jump has propagated away from the obstacle scarp and flags downflow have reoriented to parallel with the obstacle scarp. **C)** At $T = 8$ s, the flow thickening has propagated farther away and appears more strongly developed. Flags become progressively reoriented downflow of the flow thickening as it migrates away from the obstacle. **D)** At $T = 9$ s, the jump has migrated farther away from the downstream corner of the obstacle scarp than the leading corner, and flags that were originally pointing away from the lock gate have reoriented parallel to the scarp.

it had started to propagate more rapidly away from the downstream end of the scarp. After this, the front propagated at different velocities along its length with a surging behavior, but at a slower rate than that up to 7 s. After $T = 9$ s the experiment ceased as an analog to the particulate currents, because the front broke down into several bores that moved away from the scarp at around the same velocity as the propagation of the flow thickening.

The orientations of cotton flags were traced from video stills to record near-bed current vectors (Fig. 4). Before the flow body impinged on the obstacle, the flags diverged in a radial pattern from the lock with an area of parallel forward flow directly in front of the lock gate, consistent with a spreading current. During the short period ($T = 4$–6 s) when the head impinged upon and then flowed past the obstacle scarp, the flow vectors were mostly still diverging from the lock (Fig. 4A). At around $T = 6$ s, the flow had started to thicken in front of the obstacle scarp, and the thickening front had propagated a short distance from the scarp. The flow vectors between the flow-thickening front and the obstacle scarp were parallel to the scarp so that the area of thickened flow corresponded closely with that of change in flow direction (Fig. 4A). After ~ 6 s, the propagation of the flow thickening was followed by an immediate reorientation of the flags, indicating a shift in flow vector parallel to the obstacle scarp (Fig. 4 B–D). Beyond the downstream corner of the obstacle scarp the flags diverged strongly, indicating a rapid spreading of flow from this point. As the flow waned a bore (cf. Kneller et al. 1991) developed from the flow thickening and propagated farther upflow, but it did not change the orientation of the cotton flags.

Discussion of Flow Behavior

In all runs, the flow was partially blocked, with the thicker head able to move over the obstacle, but with most of the thinner body being diverted rather than flowing over the scarp. The sudden flow thickening upstream of the obstacle in these experiments is likely to be a hydraulic jump. This is based on calculations of flow Froude number from measurements of flow velocity and thickness, and flow density calculated from a prediction of sediment deposition rate (cf. Morris 1998). Estimates of velocity and thickness give Froude numbers around unity for the pre-obstacle flow body. A hydraulic jump is manifested as a standing surge or shock in the flow upper surface, accomplished by a decrease in the flow's velocity and an increase

in its thickness. It involves a change in the energy form of the current (i.e., some kinetic energy upflow of the jump is transformed into potential energy downflow of the jump). Fluid turbulence is generated by the hydraulic jump, which consists of a standing roller vortex that also engulfs ambient water and causes a loss of some of the mechanical energy of the flow (Komar 1971). This, therefore, can be an effective mechanism of flow dilution (van Andel and Komar 1969; Komar 1971). Under normal conditions, the position of the jump migrates during initial development and remains stable when the flow discharge on either side is balanced (cf. Garcia and Parker 1989). The spatial propagation of the flow-thickening front in these experiments is controlled by the discharge of the flow along the obstacle scarp. The addition of the inflowing body to the jump causes the jump to move farther away from the scarp in order to maintain the balance of discharge on either side.

Garcia and Parker (1989) and Mulder and Alexander (2001) showed experimentally that hydraulic jumps generated in steady underflows caused increased deposit thickness because of a decrease in the ratio between bed shear velocity and particle settling velocity. In natural currents, a hydraulic jump may cause preferential deposition of coarse sediment (particularly transported as bedload) when shear velocity decreases downflow of the jump (cf. Kubo and Yokokawa 2001). The initial additional turbulence generated at the hydraulic jump and ambient entrainment may prolong the suspension of finer grains, but the reduction in flow velocity across the jump may result in deposition of the suspended load more quickly because of the decay of fluid turbulence (cf. Hiscott 1994; Mulder and Alexander 2001).

Baines (1984) described experiments using an obstacle towed through a two-layer, Two-dimensional fluid (effectively the same as a gravity current flowing over a fixed obstacle) in order to investigate the magnitude of upflow disturbances. He used a Froude number, Fr, plotted against the ratio of obstacle height, Z, to flow thickness, h, to define fields of characteristic flow behavior over an obstacle for a single-layer flow. The magnitude of upflow disturbances increases rapidly with increasing obstacle height and eventually leads to complete flow blocking, and ultimately to flow reflection and reversal. According to Baines' (1984) predictions, flows with a Froude number of around unity and $Z/h \approx 0.66$ (as in our experiments) are partially blocked by the obstacle and develop a flow thickening that propagates upstream, as was observed in these experiments. The obstacle blocks the lower parts of the flows while the upper part may flow over the top of the scarp. With complete blocking the resulting flow diversion is likely to cause a greater amount of sediment to be deposited, instead of some of the current flowing over the obstacle scarp.

A gulf developed in the plan-view shape of the head of particulate flows over the obstacle but did not in the brine current. This resulted from particulate deposition in front of the obstacle reducing the negative buoyancy of the remaining flow, resulting in thinning, velocity reduction, greater blocking, and shorter runout distance. In addition, it is likely that the particulate currents were strongly stratified due to the particle settling, reducing further the ability of the body to flow over the obstacle (cf. Kneller and McCaffrey 1999). The density-stratified flow in the dense lower part of the body was deflected and the low-concentration suspension of the upper part of the flow continued forward (i.e., flow stripping).

In the brine experiment several bores were observed to detach from the area of flow thickening and move upstream (cf. Kneller et al.'s 1991 observations). Bores were not observed in the particulate flows, probably because flow deflation prevented maintenance of significant density through which bores could propagate. If low-settling-velocity particles were in suspension, such bores might develop in particulate current experiments. Laval et al. (1988) showed that particle-driven currents slow down more rapidly than brine currents of the same initial density. For brine currents the reduction in velocity is due to friction and dilution causing an increase in the volume of the surge. In particle-driven currents sediment settling is an additional factor controlling velocity. The differences between the flow behavior of the brine and particulate flows can be explained by two processes: sediment deposition and differences in mixing with ambient fluid. These differences are important because they change the flow behavior significantly at later stages of flow, and this highlights the need to for caution when applying observations from brine experiments to natural particulate flows.

The differences in flow behavior among Runs 1, 2, and 3 are due to a combination of initial flow volume and grain size of the suspended sediment. The flow thickening in Run 2 propagated farther upflow than in the equivalent experiment with coarse grain size (Run 1). This may have been due to the slower sediment fallout rate for the finer grain size, and the resulting ability for the thickened flow to sustain itself against deflation.

DEPOSITS FROM SEDIMENTARY GRAVITY CURRENTS

In the sediment-laden runs it was not possible to observe flow vectors directly within the flow and the position of the flow thickening was partly obscured by mixing of sediment into the overlying water. Despite this it is possible to relate the upstream limit of the area of thickened flow confidently with an abrupt thickening of the deposit (Figs. 3B, 5A). The abrupt thickness change decreased in magnitude around the leading corner of the obstacle, and continued with gradually decreasing amplitude from the area upstream of the scarp towards the corner of the tank beyond the lateral limit of the obstacle. It did not fully extend to the tank wall (Figs. 3B, 5A). The abrupt increase in thickness showed a small anticlockwise rotation beyond a point roughly level with the downstream corner of the obstacle and the development of a number of short, rotated sections (Fig. 5A). The abrupt increase in thickness represents the terminal position of the hydraulic jump and the maximum upstream limit of the significant influence of the obstacle on the current.

Streaks ($\sim$ 0.5 mm deep, $\sim$ 0.01 m apart) were observed on the upper surface of the deposits immediately after the currents deflated (Fig. 5A). These generally radiated from the lock gate and terminated against the abrupt increase in thickness. The angle of incidence with the abrupt increase in thickness decreased with distance away from the leading corner of the obstacle, because of the divergence of the primary flow from the lock. Furrows that are much broader than streaks occurred on the thickened deposit, and these were mainly parallel with the obstacle scarp, similar to the cotton flag orientations in the same area from the brine experiment. The streaks and furrows must have formed at a late stage in the runs, inasmuch as they occur on the upper surface of the sediment deposits.

In the area between the flow thickening and the obstacle scarp, flow vectors change during passage of the flow. The size of this area depends on the relative height of the flow body and obstacle and the flow character (cf. Baines 1984) and, in these experiments, can form a significant percentage of the area of the deposit of a particulate flow.

DISCUSSION

Flow Processes in Experimental Runs

In these experiments, the upstream line of flow thickening is interpreted as a hydraulic jump. Given that the position of a hydraulic jump remains stable when discharge on either side is balanced (Komar 1971), then the position migrates when discharge is not balanced. The areas of flow thickening migrated upstream at an angle to the obstacle scarp because of the diversion of fluid along the obstacle scarp. Following the passage of the head the incoming, nearly critical or supercritical body of the current interacted with the leading corner of the obstacle and was split either side of it, with fluid being diverted roughly parallel to the front of the obstacle scarp. A hydraulic jump formed within the body of the flow because the flow was partially blocked, and it migrated upstream directly in front of the obstacle scarp to a distance at which the discharge of incoming flow was balanced by the discharge of thickened flow to both sides of the leading

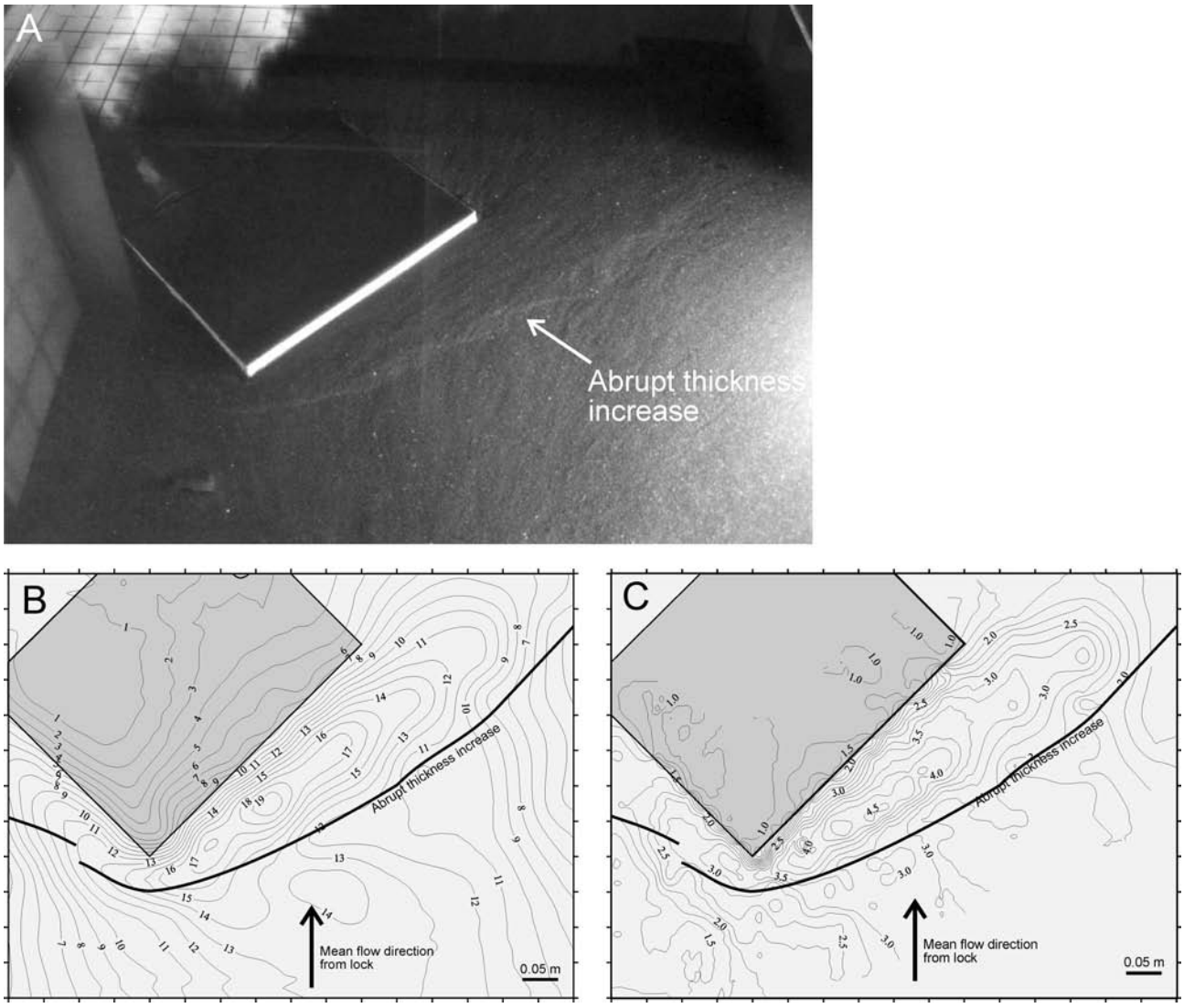

FIG. 5.—Deposit variations from a particulate flow (Run 3). **A)** Photograph showing the obstacle scarp and the abrupt thickness increase in the deposit. The obstacle and abrupt thickness increase delimit an area of thickened deposit, compared to a similar run without an obstacle. Radially spreading surface streaks in the deposit, which originate near the lock gate, terminate at the abrupt thickness increase. The abrupt thickness increase shows several distinct features: the distance between obstacle scarp and abrupt thickness increase widens, it breaks up into several segments with individual orientations greater than the overall angle of the thickness increase, and it continues in the deposit farther than the downstream corner of the scarp. **B)** Contoured sediment deposit mass (g per 25 cm^2) around the obstacle scarp in Run 3 with the position of the abrupt thickness increase superimposed. **C)** Contoured sediment deposit thickness (mm) in Run 3.

corner. The fluid diverted along the obstacle scarp from the leading corner converged with as yet unobstructed, supercritical flow coming directly from the lock. This incoming flow passed though the hydraulic jump and added to the effective discharge of the subcritical current downflow of the jump. To compensate, the hydraulic jump migrated farther upstream.

This behavior predicts that the propagation of the hydraulic jump in front of the scarp will form a straight line (represented by the dotted line in Fig. 6) assuming a constant incoming discharge per unit width across the entire length of the jump and steady flow conditions. Beyond the downstream corner of the scarp, where the flow was free to spread, the hydraulic jump is predicted to change to a more parallel-to-scarp orientation. A solid line (Fig. 6) shows the observed orientation of the abrupt thickness increase, with a characteristic curve that results from a decreasing propagation distance along the obstacle scarp. This progression towards a scarp-parallel orientation may be a further modification to flow discharge due to flow non-uniformity in the incoming body and deflation of the flow due to rapid sediment deposition downstream of the proposed hydraulic jump, as shown by the increased sediment thickness in this area. However, the flags in Run 4 show that the flow streamlines from the lock are radial and the decreasing incidence angle along the hydraulic jump towards the right-hand side of the obstacle (when observed in a down flow direction) of the incoming current may also have decreased the effective discharge in the thickened flow (Figs. 4, 6).

The disturbed flow propagated rapidly away to the right-hand side of the obstacle. This is reflected in the way that the sediment deposit is thickened, with a continuation of the abrupt thickness increase nearly to the side of the tank. The different propagation distance of the hydraulic jump between runs transporting different grain sizes indicates a difference in discharge conditions around the obstacle, because the two runs had similar forward velocities. Because only the grain size was changed, this suggests that the difference is caused by different rates of sediment deposition from the flows. Because the flows were of surge type and waned after only a few

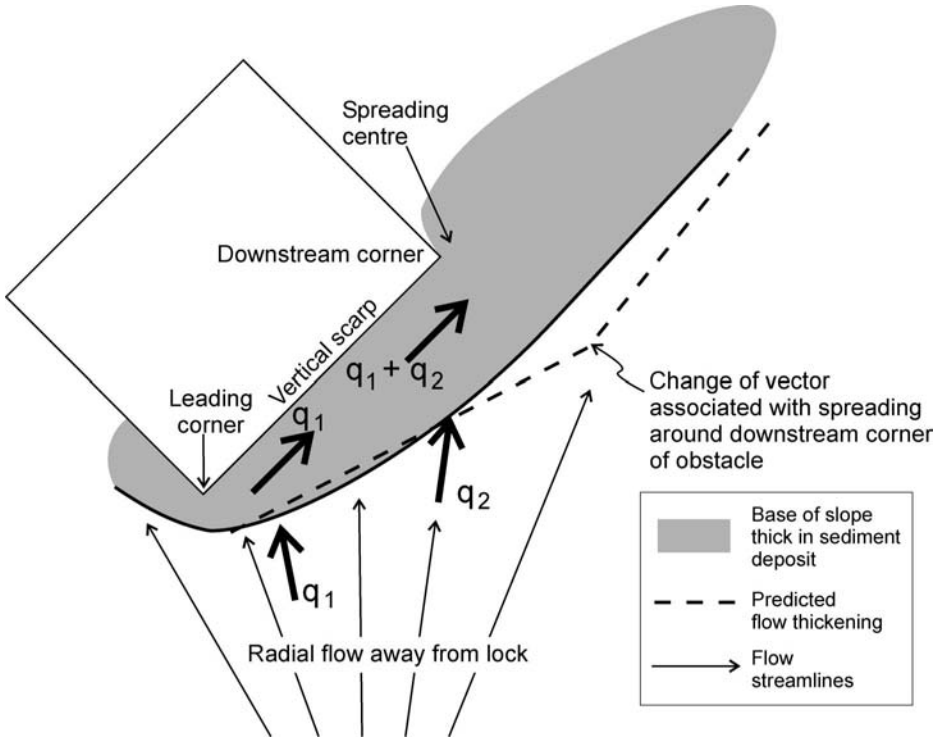

FIG. 6.—Explanation of the nonparallel propagation of a hydraulic jump away from the obstacle scarp during the period when the body of a current impinges upon the obstacle. The predicted flow thickening (dashed line) is based on addition of discharge with no adjustment for loss of discharge through deflation and deposition or increases through flow dilution. The hydraulic jump position is stable when discharge is balanced on either side and the progressive addition of current body to the thickened flow along the obstacle scarp causes the proposed hydraulic jump to migrate farther away to maintain the discharge balance. The different pattern that is observed (solid line) and the abrupt thickness increase in the deposits (shaded area) is due to further flow discharge modifications caused by rapid sediment deposition and the radial nature of the inflowing primary current.

seconds, it is not certain whether the hydraulic jump would have moved farther against the flow. However, it seems more likely that the proposed hydraulic jump may have reached an equilibrium position, where the influx of current was balanced by flow through and out the other side of the thickened flow area followed by rapid flow deflation. The presence of short, rotated segments in the abrupt increase in thickness may have resulted from the roller vortex in the hydraulic jump breaking into separate waves, which then decayed with the flow and imprinted the abrupt increase in thickness in the deposit at the end of sediment deposition.

The area between the hydraulic jump and scarp is one of *accumulative flow* (cf. Kneller and Branney 1995) in the sense that flow lines are converging, even though the radial spread of the flow upstream of the disturbance is *depletive.* Kneller and McCaffrey (1999) proposed that sites of accumulative flow (under steady conditions) were likely to be sites where reduced deposition, bypass, and even erosion may take place beneath turbidity currents. In the runs described here, the flows were accumulative but waning during deposition in front of the obstacle, and it seems likely that the effects of flow waning more than offset the effects of accumulative flow, concurring with Kneller (1995).

Implications for Turbidites

In basins where turbidity currents impinge upon obstacles that are of dimensions similar to the flow thickness, partial blocking and deflections will be important. In a natural system, the primary flow of the head may cut sole structures, creating paleocurrents radiating from the source. Following the development of a hydraulic jump and diverted flow, the primary sole structures could be overprinted by a secondary set from the deflected flow. However, the thickened and presumably slowed flow may become depositional, and the development potential of secondary sole structures is therefore questionable. Upstream of an obstacle depositional structures may have different paleocurrent directions to the primary sole structures and the divergence may be as much as 45°. Although there are differences in deposition style, it is likely that paleocurrent variations in turbidites will be similar to those seen by Kneller and McCaffrey (1999). The partial blocking of flows may produce flow stripping (cf. Piper and Normark 1983) of stratified flows, in which the lower, dense layer is confined by topography and the upper, more dilute layer is able to pass over the top.

These experiments have shown that a topographic feature can cause deposit variations directly upstream of the obstacle and to a considerable distance to the side. Turbidite thickness and facies variations could be found at distances away from relatively small obstacles in the sedimentary record. Care must be taken when interpreting the position of a paleo-obstacle from turbidite variations in two-dimensional outcrops, where the obstacle itself is not seen, because partial deflection of the flow may have taken place.

The most likely cause of partial flow blocking may be intrabasinal faults, which could provide scarp faces to act as obstacles to flow. Seabed topography produced by faults, on a scale likely to interact with turbidity currents, has been observed for example in the Gulf of Corinth (Brooks and Ferentinos 1984). However, other features on the sea floor could also cause flow disruption. Topographic features caused by salt diapirism (Kneller and McCaffrey 1995), submarine channels, or debris flows may also be enough to significantly influence turbidite facies and paleocurrent patterns.

CONCLUSIONS

Partial blocking and partial deflection of turbidity currents are important mechanisms in the interaction of turbidity currents with topography. Importantly, the experiments demonstrate that part of the body may be blocked while the head and unobstructed parts of the body continue to flow forward.

During partial deflection, the flow thickens in an area upstream of an obstacle and a hydraulic jump can form in the body of a flow, if the height of the obstacle is similar to the depth of the flow. The hydraulic jump migrates upstream to an equilibrium position at which the discharge from the incoming body is balanced by discharge in the thickened flow. The progressive addition of discharge along the length of the hydraulic jump caused by the deflection of flow causes the hydraulic jump to migrate progressively farther from the stoss of the obstacle in order to satisfy the

balanced discharge relationship. Consequently the hydraulic jump forms at an angle to an oblique obstacle.

There is a progressive change in flow vector during passage of the flow in the area upstream of an obstacle. This records an early, unobstructed, phase of flow before the current hits the obstacle, followed by a rotation due to flow deflection. Partial deflection of flow can thus explain vertical variation in paleocurrent direction in turbidites where the angle of divergence is less than about 45°.

ACKNOWLEDGMENTS

One of the experiments was run in the Earth Sciences Department of Leeds University and we are considerably grateful to Ben Kneller and Bill McCaffrey for their help with this run. Part of the laboratory work was funded by sponsorship from the former Amoco Plc, for which we particularly thank Ben Hillier. The manuscript was greatly improved following constructive reviews by Peter Haughton and David Mohrig.

REFERENCES

Agirrezabala, L.M., and García-Mondéjar, J., 1994, A coarse grained turbidite system with morpholotectonic control (Middle Albian, Ondarroa, northern Iberia): Sedimentology, v. 41, p. 383–407.

Alexander, J., and Morris, S.A., 1994, Observations on experimental non-channelized turbidites: thickness variations around obstacles: Journal of Sedimentary Petrology, v. 64, p. 899–909.

Allen, J.R.L., 1982, Sedimentary Structures; Their Character and Physical Basis, Volume II: Amsterdam, Elsevier, Developments in Sedimentology 30, 663 p.

Anderson, T.B., 1965, Turbidites whose sole markings show more than one trend—a further interpretation: Journal of Geology, v. 73, p. 812–814.

Baines, P.G., 1984, A unified description of two-layer flow over topography: Journal of Fluid Mechanics, v. 146, p. 127–167.

Brooks, M., and Ferentinos, G., 1984, Tectonics and sedimentation in the Gulf of Corinth and the Zakynthos and Kefallinia Channels, Western Greece: Tectonophysics, v. 101, p. 25–54.

Bursik, M.I., and Woods, A.W., 2000, The effects of topography on sedimentation from particle-laden turbulent density currents: Journal of Sedimentary Research, v. 70, p. 53–63.

Chikita, K.A., Smith, N.D., Yonemitsu, N., and Perez-Arlucea, M., 1996, Dynamics of sediment-laden underflows passing over a subaqueous sill: glacier-fed Peyto Lake, Alberta, Canada: Sedimentology, v. 43, p. 865–875.

Clayton, C.J., 1993, Deflection versus reflection of sediment gravity flows in the Late Llandovery Rhuddnant Grits turbidite system, Welsh Basin: Geological Society of London, Journal, v. 150, p. 819–822.

Edwards, D.A., Leeder, M.R., Best, J.L., and Pantin, H.M., 1994, On experimental reflected density currents and the interpretation of certain turbidites: Sedimentology, v. 41, p. 437–461.

Garcia, M., and Parker, G., 1989, Experiments on hydraulic jumps in turbidity currents near a canyon-fan transition: Science, v. 245, p. 393–396.

Haughton, P.D.W., 1994, Deposition of deflected and ponded turbidity currents, Sorbas Basin, Southeast Spain: Journal of Sedimentary Research, v. A64, p. 233–246.

Haughton, P.D.W., 2000, Evolving turbidite systems on a deforming basin floor, Tabernas, SE Spain: Sedimentology, v. 47, 497–518.

Hiscott, R.N., 1994, Loss of capacity, not competence, as the fundamental process governing deposition from turbidity currents: Journal of Sedimentary Research, v. A64, p. 209–214.

Hiscott, R.N., and Pickering, K.T., 1984, Reflected turbidity currents on an Ordovician basin floor, Canadian Appalachians: Nature, v. 311, p. 143–145.

Kneller, B.C., 1995, Beyond the turbidite paradigm: physical models for deposition of turbidites and their implications for reservoir prediction, *in* Hartley, A.J., and Prosser, D.J., eds., Characterization of Deep Marine Clastic Systems: Geological Society of London, Special Publication 94, p. 31–49.

Kneller, B.C., and Branney, M.J., 1995, Sustained high-density turbidity currents and the deposition of thick massive sands: Sedimentology, v. 42, p. 607–616.

Kneller, B.C., and Buckee, C., 2000, The structure and fluid mechanics of turbidity currents: a review of some recent studies and their geological implications: Sedimentology, v. 47, p. 62–94.

Kneller, B.C., and McCaffrey, W., 1995, Modelling the effects of salt-induced topography on deposition from turbidity currents, *in* Travis, C.J., Harrison, H., Hudeac, M.R., Vendeville, B.C., Peel, F.J., and Perkins, R.F., eds., Salt, Sediment and Hydrocarbons: SEPM, Gulf Coast Section, Houston, p. 137–145.

Kneller, B.C., and McCaffrey, W., 1999, Depositional effects of flow nonuniformity and stratification within turbidity currents approaching a bounding slope: deflection, reflection, and facies variation: Journal of Sedimentary Research, v. 69, p. 980–991.

Kneller, B.C., Bennett, S.J., and McCaffrey, W.D., 1995, Velocity and turbulence structure of gravity currents and internal solitary waves: potential transport and the formation of wave ripples in deep water: Sedimentary Geology, v. 112, p. 235–250.

Kneller, B.C., Edwards, D., McCaffrey, W., and Moore, R., 1991, Oblique reflection of turbidity currents: Geology, v. 14, p. 250–252.

Komar P.D., 1971, Hydraulic jumps in turbidity currents: Geological Society of America, Bulletin, v. 82, p. 1477–1488.

Kubo, Y., and Yokokawa, M., 2001, Theoretical study on breaking of waves on antidunes, *in* McCaffrey, W.D., Kneller, B.C., and Peakall, J., Particulate Gravity Currents: International Association of Sedimentologists, Special Publication 31, p. 65–70.

Laval, A., Cremer, M., Beghin, P., and Ravenne, C., 1988, Density surges: two-dimensional experiments: Sedimentology, v. 35, p. 73–84.

Lebreiro, S.M., McCave, I.N., and Weaver, P.P.E., 1997, Late Quaternary turbidite emplacement on the Horseshoe Abyssal Plain (Iberian Margin): Journal of Sedimentary Research, v. 67, p. 856–870.

Marjanac, T., 1990, Reflected sediment gravity flows and their deposits in the flysch of Middle Dalmatia, Yugoslavia: Sedimentology, v. 37, p. 921–929.

Morris, S.A., 1998, Facies variations resulting from the interaction of turbidity currents with topography [unpublished Ph.D. thesis]: Cardiff University of Wales, 384 p.

Morris, S.A., Kenyon, N.H., Limonov, A.F., and Alexander, J., 1998, Downstream changes of large-scale bedforms in turbidites around the Valencia Channel Mouth, NW Mediterranean: implications for palaeoflow reconstruction: Sedimentology, v. 45, p. 365–377.

Mulder, T., and Alexander, J., 2001, Abrupt change in slope causes variation in deposit thickness of concentrated particle-driven density currents: Marine Geology, v. 175, p. 221–235.

Pantin, H.M., and Leeder, M.R., 1987, Reverse flow in turbidity currents: the role of internal solitons: Sedimentology, v. 34, p. 1143–1156.

Pickering, K.T., and Hiscott, R.N., 1985, Contained (reflected) turbidity currents from the Middle Ordovician Cloridorme Formation, Quebec, Canada: an alternative to the antidune hypothesis: Sedimentology, v. 32, p. 373–394.

Pickering, K.T., Underwood, M.B., and Taira, A., 1992, Open-ocean to trench turbidity-current flow in the Nankai Trough: flow collapse and reflection: Geology, v. 20, p. 1099–1102.

Piper, D.J.W., and Normark, W.R., 1983, Turbidite depositional patterns and flow characteristics, Navy Submarine Fan, California Borderland: Sedimentology, v. 30, p. 681–694.

Sinclair, H.D., 1994, The Influence of lateral basinal slopes on turbidite sedimentation in the Annot Sandstones of SE France: Journal of Sedimentary Research, v. A64, p. 42–54.

Sinclair, H.D, 2000, Delta-fed turbidites infilling topographically complex basin: a new depositional model for the Annot Sandstones, SE France: Journal of Sedimentary Research, v. 70, p. 504–519.

van Andel, T.H., and Komar, P.D., 1969, Ponded sediments of the Mid-Atlantic ridge between 22° and 23° North latitude: Geological Society of America, Bulletin, v. 80, p. 1163–1190.

Woodcock, N.H., 1990, Transpressive Acadian deformation across the Central Wales Lineament: Journal of Structural Geology, v. 12, p. 329–337.

Received 17 November 2000; accepted 25 November 2002.